AJNR

Shoulder Apprehension Impacts Large-Scale Functional Brain Networks

S. Haller, G. Cunningham, A. Laedermann, J. Hofmeister, D. Van De Ville, K.-O. Lovblad and P. Hoffmeyer

AJNR Am J Neuroradiol published online 3 October 2013
http://www.ajnr.org/content/early/2013/10/03/ajnr.A3738

Published October 3, 2013 as 10.3174/ajnr.A3738

Shoulder Apprehension Impacts Large-Scale Functional Brain Networks

S. Haller, G. Cunningham, A. Laedermann, J. Hofmeister, D. Van De Ville, K.-O. Lovblad, and P. Hoffmeyer

ABSTRACT

BACKROUND AND PURPOSE: Shoulder apprehension is defined as anxiety and resistance in patients with a history of anterior glenohumeral instability. It remains unclear whether shoulder apprehension is the result of true recurrent instability or a memorized subjective sensation. We tested whether visual presentation of apprehension videos modifies functional brain networks associated with motor resistance and anxiety.

MATERIALS AND METHODS: This prospective study includes 15 consecutive right-handed male patients with shoulder apprehension (9 with right shoulder apprehension, 6 with left shoulder apprehension; 27.5 ± 6.4 years) and 10 healthy male right-handed age-matched control participants (29.0 ± 4.7 years). Multimodal MR imaging included 1) functional connectivity tensorial independent component analysis, 2) task-related general linear model analysis during visual stimulation of movies showing typical apprehension movements vs control videos, 3) voxel-based morphometry analysis of GM, and 4) tract-based spatial statistics analysis of WM.

RESULTS: Patients with shoulder apprehension had significant ($P < .05$ corrected) increase in task-correlated functional connectivity, notably in the bilateral primary sensory-motor area and dorsolateral prefrontal cortex and, to a lesser degree, the bilateral dorsomedial prefrontal cortex, anterior insula, and dorsal anterior cingulate cortex (+148% right, +144% left). Anticorrelated functional connectivity decreased in the higher-level visual and parietal areas (−185%). There were no potentially confounding structural changes in GM or WM.

CONCLUSIONS: Shoulder apprehension induces specific reorganization in apprehension-related functional connectivity of the primary sensory-motor areas (motor resistance), dorsolateral prefrontal cortex (cognitive control of motor behavior), and the dorsal anterior cingulate cortex/dorsomedial prefrontal cortex and anterior insula (anxiety and emotional regulation).

ABBREVIATIONS: dACC = dorsal anterior cingulate cortex; dlPFC = dorsolateral prefrontal cortex; dmPFC = dorsomedial prefrontal cortex; GLM = general linear model; IC = independent component; TBSS = tract-based spatial statistics; TICA = tensorial independent component analysis; VBM = voxel-based morphometry

Shoulder apprehension is defined as anxiety and resistance in patients with a history of anterior glenohumeral instability. The apprehension sign is a physical finding in which placement of the humerus in the position of abduction to 90° and maximal external rotation produces anxiety and resistance in patients with a history of anterior glenohumeral instability.[1,2]

Despite the clearly established clinical findings of shoulder apprehension, the neuronal mechanisms associated with this subjective perception of anxiety and resistance remain unexplored. In patients with recurrent complaints of persisting apprehension after surgical stabilization, it is often difficult to diagnose and appropriately address the underlying problem. Although a bony defect has been recognized as a major cause of residual instability,[3] some patients experience apprehension without any proven recurrent dislocation. It is not clear whether the origin of the complaint is true recurrent instability or whether it stems from a cerebral pattern linking a certain movement or position to a subjective sensation of apprehension. This type of apprehension could, in some cases, arise from a previously memorized unpleasant sensation associated with a particular movement or position leading to a protective reflex action, rather than being the result of true persisting instability. Failure to recognize and adequately address this issue of persisting apprehension because of cerebral patterning may result in poor outcomes and even lead to unnecessary revision surgery.

To specifically probe the neuronal activations associated with shoulder apprehension, we developed animation videos illustrat-

Received June 15, 2013; accepted after revision July 10.

From the Departments of Imaging and Medical Informatics (S.H., J.H., K.-O.L.), Orthopaedic Surgery (G.C., A.L., P.H.), and Radiology (D.V.D.V.), University Hospitals of Geneva, Geneva, Switzerland; and Institute of Bioengineering (D.V.D.V.), Ecole Polytechnique Fédérale de Lausanne, Switzerland.

Please send correspondence to PD Dr. M.Sc. Sven Haller, Service neuro-diagnostique et neuro-interventionnel DISIM, University Hospitals of Geneva, Rue Gabrielle Perret-Gentil 4, 1211 Geneva 14, Switzerland; e-mail: sven.haller@hcuge.ch

http://dx.doi.org/10.3174/ajnr.A3738

ing typical movements of shoulder apprehension and matched control videos without apprehension movements. These videos were shown during fMRI to a carefully selected group of patients with shoulder apprehension and matched healthy volunteers. Functional connectivity as well as structural changes in gray and white matter was assessed. Specifically, we addressed the hypothesis that the visual presentation of apprehension-related videos induces patterns of functional connectivity in brain networks associated with motor resistance and anxiety.

MATERIALS AND METHODS

Participants

The local institutional ethical committee approved this prospective study, and all participants gave written informed consent before inclusion. We included 15 consecutive right-handed male patients with right-sided ($n=9$) or left-sided ($n=6$) glenohumeral instability and positive shoulder apprehension test (27.5 ± 6.4 years), who were recruited during consultation by the same shoulder surgeon (A.L., 13 years of experience). They all underwent an fMRI examination before surgical shoulder stabilization by this same surgeon. Ten healthy male right-handed control-matched participants were randomly selected from the general population (29.0 ± 4.7 years, no significant difference in mean age between groups). The exclusion criteria for control patients was any history of shoulder injury or instability as well as hyperlaxity, defined as more than 85° of elbow-to-waist external rotation. All participants had normal or corrected-to-normal visual acuity, and none reported a history of major medical disorders (cancer, cardiac illness), sustained head injury, psychiatric or neurologic disorders, or alcohol or drug abuse. Participants who used psychotropics, stimulants, and β-blockers on a regular basis were excluded.

fMRI Task

The fMRI task consisted of a block-design of 2 active conditions and 1 rest condition. In the active APPREHENSION condition, self-made animation movies (10 seconds) were visually presented, including daily activities such as putting the right shoulder at risk for anteroinferior dislocation and hence triggering apprehension, for example, arming the shoulder with a javelin, quickly reaching backwards for a seatbelt, and so forth (created by C.G., 3 years of experience). The videos for the CONTROL condition presented an identical situation except for the lack of suggestive movement, which induces apprehension. After each movie, a visual analog scale was presented for 2.5 seconds, and participants rated the degree of apprehension by using a MR-compatible response box, followed by a rest period consisting of the visual presentation of a fixation cross for 17.5 seconds. The 9-point visual rating scale ranged from very unpleasant (−1) to neutral (0) to pleasant (+1). Each run consisted of 6 active and 6 control videos presented in a pseudorandomized fashion. With inclusion of the additional fixation cross-phase, each run lasted 370 seconds with each participant performing 2 runs. Before fMRI scanning, participants were familiarized with the task by using a training program outside of the fMRI scanner.

MR Imaging

MR imaging was performed on a clinical routine whole-body 3T MR scanner (Trio; Siemens, Erlangen, Germany). Functional imaging implemented a standard EPI sequence with the following fundamental parameters: 1) whole-brain coverage, 96 × 96 matrix, 39 sections, voxel size 2.3 × 2.3 × 3.3 mm^3, TE of 30 ms, TR of 2500 ms, 148 repetitions; 2) a 3D T1 sequence with the following fundamental parameters: 256 × 256 matrix, 176 sections, 1 × 1 × 1 mm^3, TE of 2.3 ms, TR of 2300 ms; and 3) a DTI sequence with the following fundamental parameters: 30 diffusion directions $b=1000$ s/mm^2 isotropically distributed on a sphere, 1 reference $b=0$ s/mm^2 image with no diffusion weighting, 128 × 128 × 64 matrix, 2 × 2 × 2 mm voxel size, TE of 92 ms, TR of 9000 ms, and 1 average.

Statistical Analysis

Statistical analysis was performed in GraphPad Prism Version 5.0 (GraphPad Software, San Diego, California; behavioral data), FSL Version 5.0.2.1 (http://fsl.fmrib.ox.ac.uk; tensorial independent component analysis [TICA], voxel-based morphometry [VBM], and tract-based spatial statistics [TBSS]), and Matlab Version R2012b (MathWorks, Natick, Massachusetts; correlation analyses) by S.H. (12 years of experience) and D.v.d.V. (14 years of experience).

Analysis of Behavioral Data

After normality testing (D'Agostino-Pearson omnibus test), the participant's age was analyzed by use of a 2-sample t test. The behavioral responses for APPREHENSION vs CONTROL for patients and control participants were analyzed by use of group-level ANOVA followed by pair-wise Bonferroni multiple comparison tests.

TICA Analysis of Functional Connectivity

Analysis was carried out by TICA[4] as implemented in MELODIC (Multivariate Exploratory Linear Decomposition into Independent Components) Version 3.10, part of FSL. The following preprocessing was applied: 1) masking of nonbrain voxels, 2) voxelwise de-meaning of the data, and 3) normalization of the voxelwise variance. Preprocessed data were whitened and projected into a 30-dimensional subspace by use of the principal component analysis (30 components by use of automatic component estimation in FSL). The whitened observations were decomposed into sets of vectors, which describe signal variation across the temporal domain (time courses), the session/participant domain, and across the spatial domain (maps) by optimization for non-Gaussian spatial source distributions by a fixed-point iteration technique.[5] Estimated component maps were divided by the standard deviation of the residual noise and thresholded by fitting a mixture model to the histogram of intensity values.[6] Three nonneurologic noise components (visual inspection, and pseudoactivation of the brain surface or vascular system) were excluded from further processing. For each of the 27 remaining independent components (ICs), the associated Smodes (which are measures of the activation strength of the component) were post hoc compared between APPREHENSION vs CONTROL by implementation of 2-sample t tests and Bonferroni correction for multiple

comparisons. The analysis was preformed 3 times: 1) right shoulder patients vs control participants, 2) left shoulder patients vs control participants, and 3) all shoulder patients vs control participants. From the 3 remaining ICs, we also post hoc identified 2 of these ICs as task positive (ICs 12 and 17), and 1 as task negative (IC 30), and correlated the combined Smodes (ie, average of Smodes of ICs 12 and 17 − Smode of IC 30) with the average behavioral responses by use of Spearman rho. The correlation coefficient was statistically evaluated by use of 2-tailed nonparametric permutation testing. It should be noted that the spatial maps of ICs 12 and 17 also contain "negative" regions (ie, dorsal anterior cingulate cortex [dACC]) that contribute as task negative.

General Linear Model Analysis of Task-Related Activation

Task-related general linear model (GLM) data processing was carried out by use of FEAT (fMRI Expert Analysis Tool) Version 5.98, part of FSL. At the first level, the contrast of APPREHENSION vs CONTROL (and the inverse comparison) was calculated separately for each run of each participant. At the second level, the intraparticipant difference in the 2 runs of APPREHENSION vs CONTROL (and the inverse comparison) was assessed individually. At the third level, the group difference between all 15 patients and 10 control participants was calculated. We carried out higher-level analysis by using a fixed-effects model, forcing the random-effects variance to zero in FLAME (FMRIB Local Analysis of Mixed Effects).[7-9] Z (Gaussianized T/F)-statistic images were thresholded by use of clusters determined by $Z > 2.3$ and a corrected cluster significance threshold of $P = .05$.

Gray Matter VBM Analysis of T1 Data

The VBM analysis was analyzed by use of the FSL software package (Version 5.0.2.1). Standard processing steps were used, as described previously.[10,11] The essential processing steps included brain extraction in BET (Brain Extraction Tool, part of FSL), tissue-type segmentation by FAST4 (part of FSL), nonlinear transformation into Montreal Neurological Institute reference space, and creation of a study-specific GM template. The native GM images were then nonlinearly re-registered to this template. The modulated segmented images were then smoothed with an isotropic Gaussian kernel with a sigma of 2 mm. Finally, we applied voxelwise GLM by using permutation-based nonparametric testing (Randomise, part of FSL), correcting for multiple comparisons implementing threshold-free cluster enhancement.[12] Fully corrected P values $< .05$ are considered as significant. Similar to the TICA analysis above, this analysis was repeated for right shoulder patients vs control participants, left shoulder patients vs control participants, and all shoulder patients vs control participants.

White Matter TBSS Analysis of DTI Data

The TBSS analysis of the DTI data was again done implementing the FSL software package (Version 5.0.2.1), according to the standard procedure described in detail.[13] In principle, TBSS projects all participants' fractional anisotropy data onto a mean fractional anisotropy tract skeleton by using nonlinear registration. The tract skeleton is the basis for voxelwise cross-participant statistics and reduces potential misregistrations as the source for false-positive or false-negative results. Equivalent to the VBM analysis discussed above, we performed voxelwise statistical analysis with threshold-free cluster enhancement[12] correction for multiple comparisons, considering fully corrected P values $< .05$ as significant. Again, analysis was repeated for right shoulder patients vs control participants, left shoulder patients vs control participants, and all shoulder patients vs control participants.

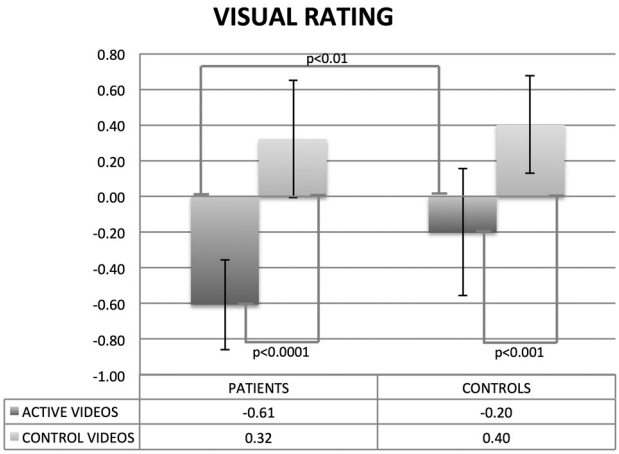

FIG 1. Visual rating ranging from unpleasant (−1) to pleasant (+1) associated with the presentation of APPREHENSION and CONTROL videos for patients and healthy volunteers. APPREHENSION vs CONTROL videos were associated with reduced rating values for both groups ($P < .0001$ corrected patients; $P < .001$ corrected control volunteers). APPREHENSION videos were associated with lower rating scores when comparing patients vs healthy volunteers ($P < .01$ corrected), whereas there was no significant effect for CONTROL videos.

RESULTS

Behavioral Data

In both patients and healthy volunteers, the APPREHENSION videos induced significantly increased ($P < .001$ corrected patients; $P < .01$ corrected control volunteers) unpleasant ratings compared with CONTROL videos. Moreover, when we compared patients vs healthy control participants, only the APPREHENSION videos ($P < .01$ corrected), but not the CONTROL videos, yielded more unpleasant ratings in patients vs control volunteers (Fig 1). These results confirm that our experimental setup induces subjective perception of unpleasantness associated with the visual perception of our shoulder apprehension movies in both patients and control participants. It also demonstrates that patients had significantly more unpleasant ratings for APPREHENSION videos vs CONTROL videos compared with matched-control participants.

Functional Connectivity fMRI Activations

The independent component analysis yielded 3 task-related ICs with a significant ($P < .05$ corrected) difference in Smode (a measure of the activation strength of the ICs) for patients compared with control participants. All 3 ICs were significant for all patients vs control participants and right shoulder patients vs control participants. In addition, IC 17 was significant for left shoulder patients vs control participants, whereas the other 2 components showed a clear equivalent but just a nonsignificant trend. It is noteworthy that there was a higher number of right vs left shoul-

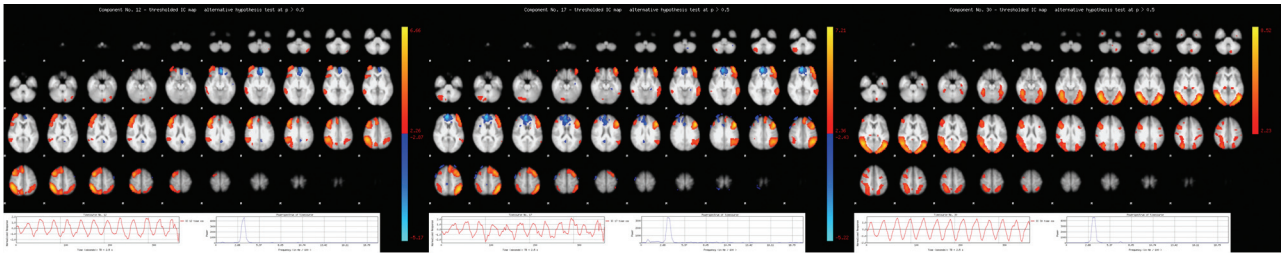

FIG 2. Patients vs control participants had a significantly ($P < .05$ corrected) higher task-correlated functional connectivity in 2 almost mirror symmetric components (IC 12 + 148% Smode in the right hemisphere; IC 17 + 144% Smode in left hemisphere). These networks include the primary sensory-motor areas compatible with motor resistance, dlPFC associated with cognitive control of motor behavior and dACC/dmPFC associated with emotional regulation. In contrast, patients had significantly reduced functional connectivity in a bilateral higher-level visual and parietal network (IC 30 −185% Smode). Moreover, this component is anticorrelated with the video presentation, in contrast to the components IC 12 and IC 17. Axial sections of the spatial representation of the ICs 12, 17, and 30 are illustrated at the top. The inserts at the bottom represent the average time courses of these ICs (left) and the corresponding Fourier spectra (right).

der patients, which explains this higher level of significance. There was no significant difference between right vs left shoulder patients. Therefore, we report the following results for all patients vs control participants.

Patients vs control participants had a significantly ($P < .05$ corrected) higher functional connectivity in 2 almost-mirror symmetric components, notably in the bilateral primary sensory-motor area and dorsolateral prefrontal cortex (dlPFC), bilateral dorsomedial prefrontal cortex (dmPFC), anterior insula, and dACC (+148% SMode in right hemisphere IC 12, and +144% Smode in left hemisphere IC 17). In contrast, patients had significantly reduced functional connectivity in a bilateral higher-level visual network including the parietal region (−185% Smode IC 30) (Fig 2).

The additionally performed correlation between task-positive minus task-negative Smodes and behavioral ratings revealed a significant negative correlation (rho = −0.47, $P = .02$) for all participants, and trends within the populations (rho = −0.63, $P = .05$ in control participants and rho = −0.31, $P = .27$ in patients).

These correlations indicate increasing functional connectivity activation strength in task-positive networks with increasing unpleasantness (Fig 3).

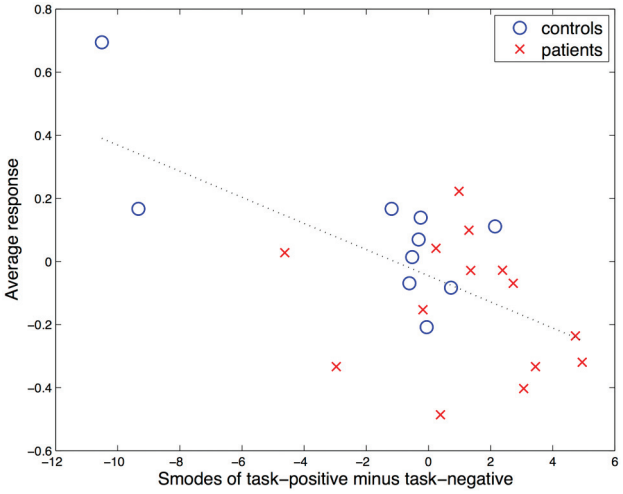

FIG 3. Correlation analysis between the Smodes (measure of activation strength) of task-positive (ICs 12 and 17) minus task-negative (IC 30) networks, and the participant average behavioral rating of unpleasantness. The negative correlation (rho = −0.4687) was significant ($P = .022$). Red "x" indicates individual patients; blue "o" indicates individual healthy volunteer data.

GLM Analysis of Task-Related Activation

The task-related GLM analysis revealed activation in the left primary sensory-motor area and dlPFC, which overlaps with IC 17, yet at a lower degree of significance. The corresponding contralateral regions showed a clear trend, which remained just below the multiple comparisons corrected threshold (Fig 4).

VBM Analysis of Gray Matter and TBSS Analysis of White Matter

The VBM analysis of GM as well as the TBSS analysis of WM revealed no differences between groups.

DISCUSSION

Patients with shoulder apprehension have increased functional connectivity in the primary sensory-motor areas compatible with motor resistance, dlPFC associated with cognitive control of motor behavior, and the dACC/dmPFC and anterior insula associated with anxiety and emotional regulation, despite the absence of potentially confounding structural alterations.

The current investigation is based on the observation that functional connectivity is not stationary but is variable with time. Functional connectivity may change spontaneously,[14] by exogenous stimulation,[15] or by learning.[16-18] Therefore, we exposed participants to videos of situations, which typically induce apprehension, to modulate functional connectivity related to the perception of apprehension. Our approach thus differs from "classic" resting-state fMRI studies without any specific task.[19,20] It is noteworthy that this change in paradigm is essential for the current investigation, as we only expect subtle changes at baseline in "classic" resting-state fMRI of apprehension patients who have no cognitive impairments. The presentation of apprehension videos is thus necessary to induce functional connectivity associated with the perception and, more generally, the processing of shoulder apprehension.

The functional connectivity was increased in patients vs volunteers by approximately 145% in the bilateral primary motor and sensory areas, as well as the bilateral dlPFC. It is interesting to note that during the shoulder apprehension test,[1,2] patients had an increased muscle tone and resistance in response to external rotation of the shoulder. Our findings of increased functional

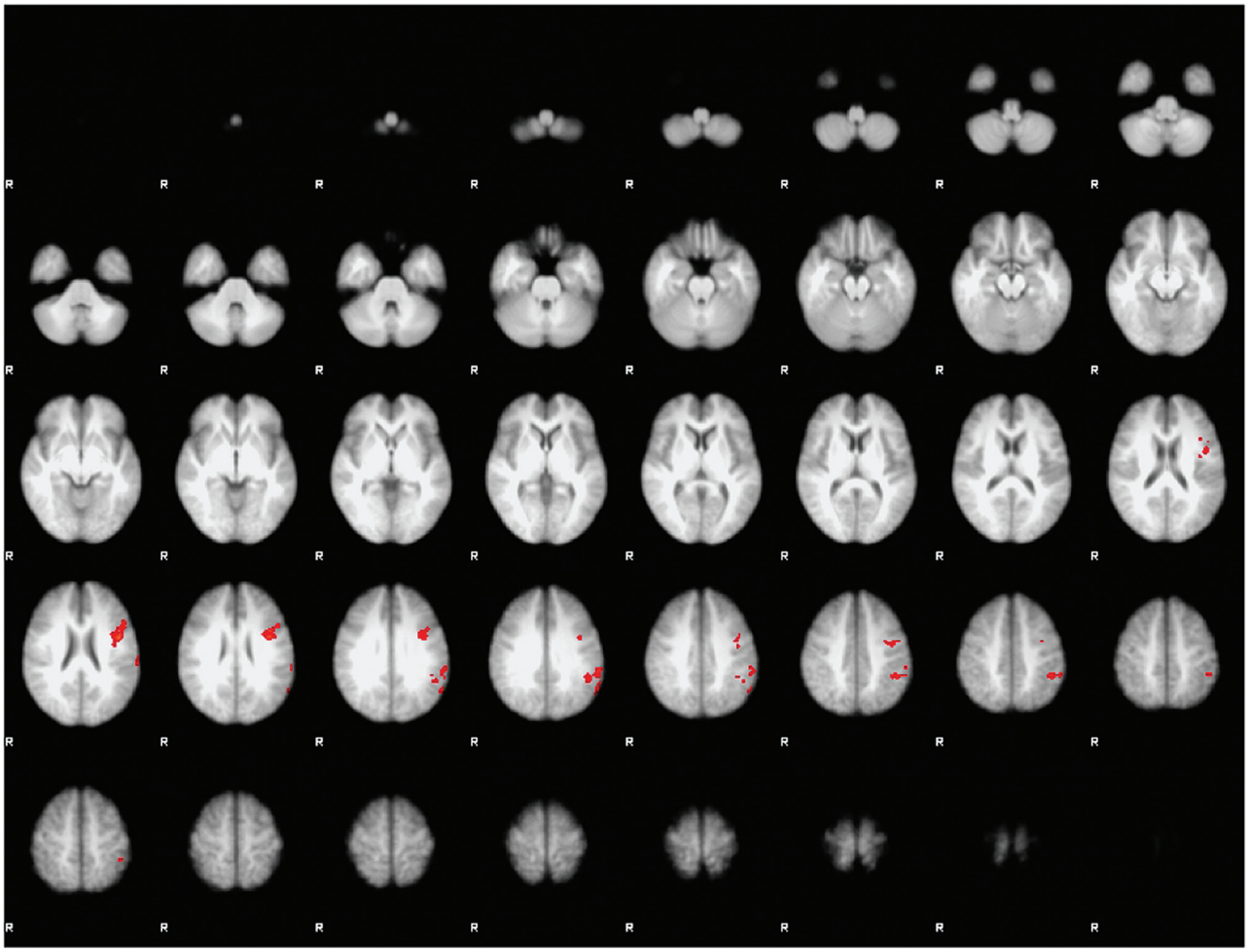

FIG 4. Hypothesis-driven GLM analysis for contrast of APPREHENSION videos vs CONTROL videos. Patients vs healthy volunteers had increased activation in the left primary sensory-motor area and dlPFC overlapping with IC 17, yet at a lower degree of significance. The corresponding contralateral regions showed a clear trend, which remained just below multiple comparisons corrected threshold (not shown). The inverse comparison of healthy volunteers vs patients yielded no significant differences.

connectivity in the primary sensory-motor area as well as in the dlPFC, which is consistently involved in the cognitive control of motor behavior,[21] are consistent with a preparation or readiness activation of the motor system in muscular resistance. Moreover, Hamilton et al[22] and Korgaonkar et al[23] propose the dlPFC is involved in the appraisal of negative emotional inputs (appraisal being deregulated in major depressive disorder). In the context of our shoulder apprehension videos, the increase in dlPFC might indicate an increased reappraisal of negative information related to the negative valence of the videos, in addition to its role in modulating pre/motor regions.

In addition, we observed an increase in functional connectivity in the dmPFC, dACC, and anterior insula. These regions are consistently involved in emotional regulation (http://neurosynth.org/terms/emotion, http://neurosynth.org/terms/regulation) and anxiety (http://neurosynth.org/terms/anxiety). Although no previous imaging study specifically addressed apprehension, we consider anxiety and fear as key cognitive processes associated with shoulder apprehension. A recent meta-analysis of instructed fear studies concludes that the dACC/dmPFC is a part of a "core" fear network, which is activated irrespective of how fear was learned.[24] One study assessed anticipatory anxiety in participants with spider phobia[25] and identified increased activation notably in the dACC/dmPFC and insula in spider phobics compared with volunteers while anticipating phobic stimulation. Another study assessed anticipation of interoceptive threat in 15 participants reporting high vs 14 participants reporting low fear.[26] Participants were trained that 1 of 2 cues predicted the occurrence of a hyperventilation task, which reliably produced body symptoms in all participants. The comparison of high-fear vs low-fear groups during the anticipation period, again, activated the dACC/dmPFC and bilateral anterior insula. Moreover, anticipatory anxiety was assessed in 14 healthy volunteers.[27] The paradigm consisted of a visual presentation of blue circles associated with a certain likelihood of aversive transcutaneous electrical nerve stimulations vs visual presentation of red circles without painful stimuli. Again, anticipatory anxiety was associated with activations in the bilateral anterior insula and midline frontal cortex (overlapping with the dACC/dmPFC). Spider phobia, hyperventilation, and transcutaneous electrical nerve stimulations as aversive stimuli evidently differ from shoulder apprehension in our current investigation. Nevertheless, the anticipatory anxiety in the discussed studies is an essential cognitive process involved in shoulder apprehension. In a consistent fashion, the reported activations of

these above-mentioned studies remarkably overlap with parts of the observed upregulated networks of our current investigation. This finding is remarkable, as the above-mentioned fMRI studies used hypothesis-driven data analyses, whereas our current investigation implemented a hypothesis-free independent component analysis. Only 1 previous study assessed functional connectivity in anticipatory anxiety; however, it implemented a fundamentally different region-of-interest approach.[28] This study included 14 anxiety-positive and 14 anxiety-normative participants performing an affective picture anticipation task. In a first step, activation in the bilateral anterior insula was identified in a task-related analysis, replicating the results of the task-related anticipatory anxiety studies discussed above. In a second step, functional connectivity was calculated with the left and right anterior insula as a seed region—in contrast to the exploratory independent component analysis of our current study, which assessed the entire brain without predefined seed regions. Nevertheless, the bilateral anterior insula in the anxiety-positive group overlap considerably with the networks identified in our study.

It is worthwhile emphasizing that the alterations in functional connectivity in the current investigation were identified by use of data-driven IC analysis without prior assumptions. Nevertheless, the observed changes in functional connectivity are by no means random yet very meaningful in the context of shoulder apprehension, as discussed above. The relevance of these task-correlated networks is further supported by the additionally performed hypothesis-driven GLM analysis, which demonstrated overlapping activations in the left sensory-motor areas and dlPFC as well as a clear and almost significant trend in the contralateral areas. That the functional-connectivity TICA analysis is more sensitive compared with the task-related GLM analysis can be explained by the fact that GLM requires strict multiple-comparisons correction of approximately 100,000 voxels instead of only 30 ICs. In addition, TICA averages signal across multiple voxels, thereby increasing the signal-to-noise ratio compared with the single-voxel GLM analysis.

Moreover, the significant correlation between ratings and functional activation strengths revealed that task-positive networks, including the sensory-motor area, dlPFC, and dACC/dmPFC, are activated more strongly during the processing of unpleasant experiences. In contrast, the task-negative higher-level visual networks are less activated in subsequent resting blocks. Therefore, shoulder apprehension progressively disturbs the balance between task-positive and task-negative networks as unpleasantness increases. Correspondingly, delayed recovery of resting-state activity in regions of the default mode network has also been reported after exposure to unpleasant visual movie fragments[29] or after a demanding cognitive task such as regulation by use of real-time fMRI neurofeedback.[30] These findings not only show the direct implication of shoulder apprehension and the motor networks but also show brain processes likely to be related to interoceptive awareness, anxiety, and emotional regulation.

Strengths and Limitations

Strengths of our current investigation are the strict patient selection, the complementary analyses of functional connectivity and task-related fMRI, and the exclusion of potentially confounding morphometric changes in both GM and WM. However, several limitations should be considered. First, the study group was small and was limited to men. Second, to increase the number of patients, we grouped together those with left and right shoulder instability, as we assumed that the cognitive processes related to apprehension were global and did not depend on the side of shoulder instability. Accordingly, we could not observe differences between patients with left shoulder instability vs control participants or those patients with right shoulder instability vs control participants, nor in the direct comparison between patients with left vs right shoulder apprehension. Third, we investigated only shoulder apprehension. We assumed that the neuronal activations associated with apprehension and anxiety were not limited to shoulder apprehension, but a general effect of apprehension including, for example, knee instability; this remains to be elucidated in future studies. Finally, we assumed that apprehension is a dynamic process, which may change with time (eg, after shoulder stabilization). In this investigation, we only assessed the phase of apprehension in patients with acute shoulder instability. Longitudinal assessment of patients with shoulder apprehension would be most interesting because the dynamic installation of apprehension-related changes in brain activations could be assessed, as well as modifications in brain activations with time associated with different treatment strategies in the sense of a surrogate marker.

CONCLUSIONS

Although shoulder apprehension is a well-known problem in sports medicine, the underlying mechanisms remain poorly understood. We demonstrate changes in neuronal processing associated with shoulder apprehension, indicating that apprehension is more complex than a pure mechanical problem of the shoulder. This also explains why mechanical stabilization alone oftentimes provides unsatisfactory results.

Disclosures: Sven Haller—*UNRELATED: Grants/Grants Pending:* Swiss National Science Foundation,* Comments: Principal investigator (SNF project 320030_147126/1), not related to this work; Dimitri Van De Ville—*UNRELATED: Grant:* Swiss National Science Foundation,* Comments: under grant PP00P2–123438 (salary DVDV). Pierre Hoffmeyer—*UNRELATED: Travel/Accommodations/Meeting Expenses Unrelated to Activities Listed:* Academic meetings (American Academy of Orthopaedic Surgeons [AAOS], European Federation of National Associations of Orthopaedics and Traumatology [EFORT], Swiss Society of Orthopaedic Surgery and Traumatology [SSOT]),* Comments: Institution funds travel and accommodations for scientific meetings. **Money paid to institution.*

REFERENCES

1. Rowe CR, Zarins B. **Recurrent transient subluxation of the shoulder.** *J Bone Joint Surg Am* 1981;63:863–72
2. Jobe FW, Kvitne RS, Giangarra CE. **Shoulder pain in the overhand or throwing athlete. The relationship of anterior instability and rotator cuff impingement.** *Orthop Rev* 1989;18:963–75
3. Burkhart SS, De Beer JF. **Traumatic glenohumeral bone defects and their relationship to failure of arthroscopic Bankart repairs: significance of the inverted-pear glenoid and the humeral engaging Hill-Sachs lesion.** *Arthroscopy* 2000;16:677–94
4. Beckmann CF, Smith SM. **Tensorial extensions of independent component analysis for multisubject fMRI analysis.** *Neuroimage* 2005;25:294–311
5. Hyvärinen A. **Fast and robust fixed-point algorithms for independent component analysis.** *IEEE Trans Neural Netw* 1999;10:626–34
6. Beckmann CF, Smith SM. **Probabilistic independent component**

analysis for functional magnetic resonance imaging. *IEEE Trans Med Imaging* 2004;23:137–52
7. Beckmann CF, Jenkinson M, Smith SM. **General multilevel linear modeling for group analysis in fMRI.** *Neuroimage* 2003;20:1052–63
8. Woolrich MW, Behrens TE, Beckmann CF, et al. **Multilevel linear modelling for fMRI group analysis using Bayesian inference.** *Neuroimage* 2004;21:1732–47
9. Woolrich M. **Robust group analysis using outlier inference.** *Neuroimage* 2008;41:286–301
10. Smith SM, Jenkinson M, Johansen-Berg H, et al. **Tract-based spatial statistics: voxelwise analysis of multi-subject diffusion data.** *Neuroimage* 2006;31:1487–505
11. Smith SM, Johansen-Berg H, Jenkinson M, et al. **Acquisition and voxelwise analysis of multi-subject diffusion data with tract-based spatial statistics.** *Nat Protoc* 2007;2:499–503
12. Smith SM, Nichols TE. **Threshold-free cluster enhancement: addressing problems of smoothing, threshold dependence and localisation in cluster inference.** *Neuroimage* 2009;44:83–98
13. Smith SM, Jenkinson M, Woolrich MW, et al. **Advances in functional and structural MR image analysis and implementation as FSL.** *Neuroimage* 2004;23 Suppl 1:S208–19
14. Raichle ME. **Two views of brain function.** *Trends Cogn Sci* 2010;14:180–90
15. Büchel C, Coull JT, Friston KJ. **The predictive value of changes in effective connectivity for human learning.** *Science* 1999;283:1538–41
16. Bassett DS, Wymbs NF, Porter MA, et al. **Dynamic reconfiguration of human brain networks during learning.** *Proc Natl Acad Sci U S A* 2011;108:7641–46
17. Lewis CM, Baldassarre A, Committeri G, et al. **Learning sculpts the spontaneous activity of the resting human brain.** *Proc Natl Acad Sci U S A* 2009;106:17558–63
18. Haller S, Kopel R, Jhooti P, et al. **Dynamic reconfiguration of human brain functional networks through neurofeedback.** *Neuroimage* 2013;81C:243–52
19. Greicius MD, Krasnow B, Reiss AL, et al. **Functional connectivity in the resting brain: a network analysis of the default mode hypothesis.** *Proc Natl Acad Sci U S A* 2003;100:253–58
20. Damoiseaux JS, Rombouts SA, Barkhof F, et al. **Consistent resting-state networks across healthy subjects.** *Proc Natl Acad Sci U S A* 2006;103:13848–53
21. Cieslik EC, Zilles K, Caspers S, et al. **Is there "one" DLPFC in cognitive action control? Evidence for heterogeneity from co-activation-based parcellation.** *Cereb Cortex* 2012 Aug 23. [Epub ahead of print]
22. Hamilton JP, Etkin A, Furman DJ, et al. **Functional neuroimaging of major depressive disorder: a meta-analysis and new integration of base line activation and neural response data.** *Am J Psychiatry* 2012;169:693–703
23. Korgaonkar MS, Grieve SM, Etkin A, et al. **Using standardized fMRI protocols to identify patterns of prefrontal circuit dysregulation that are common and specific to cognitive and emotional tasks in major depressive disorder: first wave results from the iSPOT-D study.** *Neuropsychopharmacology* 2013;38:863–71
24. Mechias ML, Etkin A, Kalisch R. **A meta-analysis of instructed fear studies: implications for conscious appraisal of threat.** *Neuroimage* 2010;49:1760–68
25. Straube T, Mentzel HJ, Miltner WH. **Waiting for spiders: brain activation during anticipatory anxiety in spider phobics.** *Neuroimage* 2007;37:1427–36
26. Holtz K, Pané-Farré CA, Wendt J, et al. **Brain activation during anticipation of interoceptive threat.** *Neuroimage* 2012;61:857–65
27. Schunck T, Erb G, Mathis A, et al. **Test-retest reliability of a functional MRI anticipatory anxiety paradigm in healthy volunteers.** *J Magn Reson Imaging* 2008;27:459–68
28. Simmons AN, Stein MB, Strigo IA, et al. **Anxiety positive subjects show altered processing in the anterior insula during anticipation of negative stimuli.** *Hum Brain Mapp* 2011;32:1836–46
29. Eryilmaz H, Van De Ville D, Schwartz S, et al. **Impact of transient emotions on functional connectivity during subsequent resting state: a wavelet correlation approach.** *Neuroimage* 2011;54:2481–91
30. Van De Ville D, Jhooti P, Haas T, et al. **Recovery of the default mode network after demanding neurofeedback training occurs in spatio-temporally segregated subnetworks.** *Neuroimage* 2012;63:1775–81